

Collinear and non-collinear spin ground state of wurtzite CoO

Myung Joon Han,^{1,2,*} Heung-Sik Kim,¹ Dong Geun Kim,³ and Jaejun Yu^{3,†}

¹*Department of Physics, Korea Advanced Institute
of Science and Technology, Daejeon 305-701, Korea*

²*KAIST Institute for the NanoCentury, KAIST, Daejeon 305-701, Korea*

³*Department of Physics and Astronomy, CSCMR,
Seoul National University, Seoul 151-747, Korea*

(Dated: June 7, 2022)

Abstract

Collinear and non-collinear spin structures of wurtzite phase CoO often appearing in nano-sized samples are investigated using first-principles density functional theory calculations. We examined the total energy of several different spin configurations, electronic structure and the effective magnetic coupling strengths. It is shown that the AF3-type antiferromagnetic ordering is energetically most stable among possible collinear configurations. Further, we found that a novel spiral spin order can be stabilized by including the relativistic spin-orbit coupling and the non-collinearity of spin direction. Our result suggests that a non-collinear spin ground state can be observed in the transition-metal-oxide nanostructures which adds an interesting new aspect to the nano-magnetism study.

PACS numbers: 75.75.-c, 71.15.Mb, 75.30.Et

*Electronic address: mj.han@kaist.ac.kr

†Electronic address: jyu@snu.ac.kr

I. INTRODUCTION

Recently transition-metal-oxide (TMO) nanocrystals have generated considerable research interest due to their intriguing material properties and their potential applications such as storage device and catalysis [1–15]. Nano-sized TMO crystals often exhibit different material characteristics from its bulk counterpart. For example, unusual magnetic signals have been reported in MnO nanoparticles [7–10], while bulk MnO is known to be antiferromagnetic (AFM). The reduced coordination number for the metal ion at its surface probably affects the electronic structure of nano-sized TMO [9, 11]. Furthermore, TMO nanocrystals often exhibit unconventional structural properties which are not found in bulk [12–15]. Wurtzite (WZ) CoO is one of the examples. Several experiments independently reported that WZ phase of CoO is stabilized at the nano-meter scale although the bulk phase CoO has the rock-salt (RS) structure [13–15].

The magnetic property of WZ CoO is particularly interesting especially after room temperature ferromagnetism was found in the Co-doped ZnO [16–18]. The origin of ferromagnetic signals in the Co-doped ZnO is still under debate, whereas some experimental efforts have failed to observe the room temperature ferromagnetism [19, 20]. Since ZnO has a WZ structure and doped-Co ions most likely substitute for Zn, the spin structure of WZ CoO can have important implications for the magnetic property of Co-doped ZnO.

In spite of previous efforts, the magnetic properties of WZ CoO are still not clearly understood. An early *ab-initio* calculation based on the local (spin) density approximation (L(S)DA) [14] was followed by a LDA+U (LDA plus Hubbard U) study which predicts an AFM spin ground state with a finite gap [21]. By using Monte Carlo simulations, Archer *et al.* also reported AFM spin ordering and estimated the spin exchange constants as well as the magnetic transition temperatures [22]. In a more recent study, Hanafin *et al.* studied the shape dependence of the magnetism of WZ CoO nanoparticles by simulating the Heisenberg spin hamiltonian [23]. They performed an extensive Monte Carlo simulation based on exchange coupling constants obtained from Ref. 22. Importantly, however, the ground state spin configuration of the WZ CoO has not yet been fully explored, and it still remains unclear. For example, within the collinear spin picture, there may exist several AFM spin arrangements other than the *c*-type AFM order. Moreover, it is important in the surface-rich nanocrystals to include the relativistic spin-orbit couplings. The inclusion of

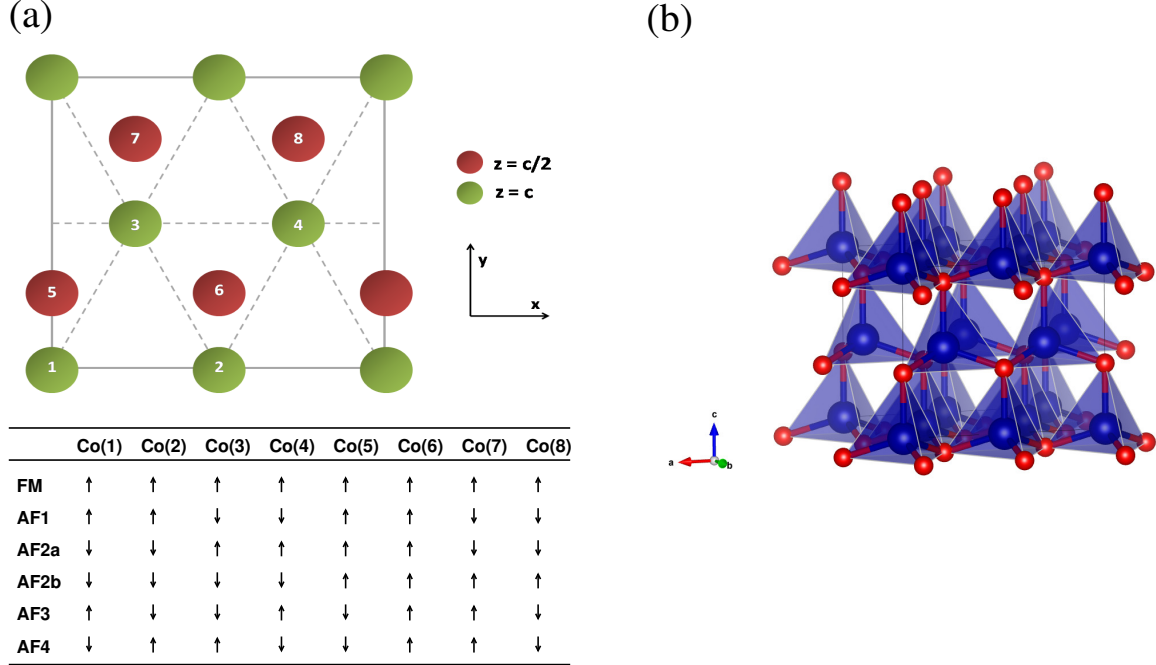


FIG. 1: (Color online) (a) Possible spin structures within the sixteen-atom unit cell. The upper part: the bright (green) and dark (red) circles represent Co atoms at $z = 0, c$ and $z = \frac{1}{2}c$ plane, respectively. The lower part: up/down arrows depict up/down spins, respectively. (b) The ball-and-stick figure for the unit cell. The larger and smaller balls represent Co and O atoms, respectively.

these effects combined with AFM coupling can lead to a novel non-collinear spin structure stabilized in TMO nanocrystals.

In this paper, we investigated the magnetic properties of WZ CoO in detail for the case of non-collinear as well as collinear spin. The electronic structure and exchange interaction are also investigated. Within the collinear spin case, one of the AFM spin orderings, so-called AF3 order, is shown to be most stable energetically, and is different from c -type AFM order. Fully relativistic calculations show that non-collinear spin configurations may be more stable than collinear ones. All possible spin configurations were investigated within sixteen-atom unitcell for the collinear case and twenty-four-atom unitcell for the non-collinear case. Our results suggest that a novel spiral spin structure can be realized in CoO nanocrystals, demonstrating that CoO is a very unique example in the study of nano-magnetism. That is, the nano-size effect stabilizes a different structural phase and leads to a novel magnetic ground state in the nano-meter scale.

II. COMPUTATIONAL DETAILS

We carried out density functional theory (DFT) calculations for the periodic unit cell within LDA+ U [24] method by employing a linear combination of localized pseudo-atomic orbitals method [25]. The effective Coulomb interaction parameter $U_{eff} = U - J$ is taken as 6 eV, which is proven to be reasonable for the calculation of RS CoO [26] while the results of other U values will also be discussed in the following section. Ceperley-Alder exchange-correlation energy functional as parameterized by Perdew and Zunger has been adopted [27]. Our basis orbitals were generated by a confinement potential scheme [25] with cutoff radii of 4.5 a.u. and 5.5 a.u. for O and Co, respectively. Troullier-Martins type pseudo-potentials [28] with a partial core correction [29] were used to replace the deep core potentials by norm-conserving soft potentials in a factorized separable form with multiple projectors proposed by Blöchl [30]. In this pseudo-potential generation, the semi-core $3p$ electrons for Co atoms were included as valence electrons in order to take into account the contribution of the semi-core states to the electronic structures. Real-space grid techniques [31] were used with an energy cutoff of 220 Ry in numerical integrations. In addition, the projector expansion method was employed to accurately calculate three-center integrals associated with a deep neutral atom potential [32]. For lattice parameters, we consider the experimental values of a WZ CoO nanorod, prepared by the thermal decomposition of a cobalt-oleate complex: $a = 3.249 \text{ \AA}$ and $c = 5.206 \text{ \AA}$ [15], which are consistent with the values reported by Seo *et al.* [13]. For non-collinear calculations, we generated j -dependent pseudopotential, by solving the Dirac equation instead of the conventional Schrödinger equation, in which the fully relativistic effect as well as the spin-orbit coupling terms were included [33]. In this computation scheme, the spins are represented by a spinor matrix, and therefore, the angles between Co spins can have arbitrary values [34].

III. RESULT AND DISCUSSION

Figure 1(a) shows the six possible collinear spin structures within the sixteen-atom unit-cell adapted in this study where the dark (red) and bright (green) spheres represent Co atoms at $z = c/2$ and $z = c$, respectively. The up/down spins are depicted by up/down arrows in the lower part of Fig. 1(a). The ball-and-stick figure for the unitcell is presented

	AFM (in)	FM (in)	AFM (out)	FM (out)	E_{tot}
FM	0	6	0	6	0.072
AF1	4	2	4	2	0.002
AF2a	4	2	2	4	0.010
AF2b	0	6	6	0	0.041
AF3	4	2	4	2	0.000
AF4	4	2	2	4	0.009

TABLE I: Total number of AFM and FM couplings and the calculated total energies for six different collinear spin configurations (in the unit of eV/CoO). The terms ‘in’ and ‘out’ refer to the number of nearest couplings along the ‘in-plane’ and ‘out-of-plane’ directions, respectively. The energy of the most stable AF3 is set to be zero.

in Fig. 1(b). In addition to the ferromagnetic (FM) order, five different AFM configurations can be considered, namely AF1, AF2a, AF2b, AF3, and AF4 [35]. The calculated total energies (E_{tot}) are presented in Table I where E_{tot} of AF3 is set to be zero. The results show that AF3 is stabler than any other AFM phases by 0.002–0.041 eV/CoO and than FM by 0.072 eV/CoO. This order of stability among the spin configurations is found to be robust against U -value. The calculations with $U=4$ and 8 eV show that the deviations in the calculated E_{tot} relative to AF3 can be different by $\sim 15\text{--}25\%$ and the order of E_{tot} remains same with $U=6$ eV result. Since the ground state spin configuration is AFM, our result implies that the magnetic signal previously detected by X-ray magnetic circular dichroism (XMCD) measurement [15] is not attributed to WZ phase of CoO although the contribution from the uncompensated surface moments cannot be ruled out [22]. Also, the room temperature ferromagnetism observed in Co-doped ZnO is not likely an intrinsic effect from the ferromagnetic ordering of Co spins, as concluded by recent Monte Carlo simulations [23].

Note that AF2b corresponds to the c -type AFM order that was studied by Risbud *et al.* within LSDA ($U = 0$) [14] and by two of the authors of this paper within LDA+ U [21]. While AF2b is more stable than FM [21], its total energy is notably higher than the other AFM configurations. The c -type AFM order is therefore not the ground state configuration (even among the collinear spin structures) and cannot be realized in the experimental situation.

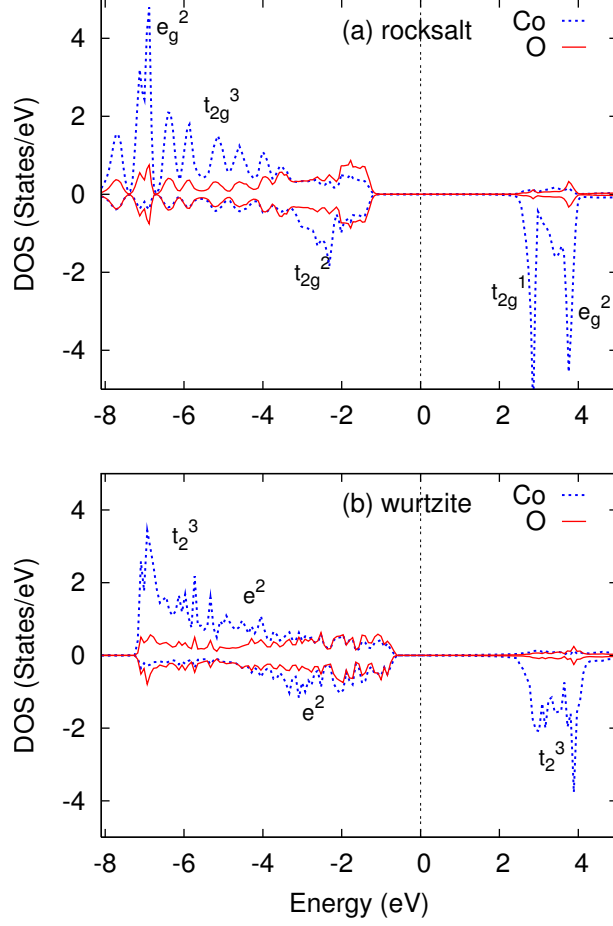


FIG. 2: (Color online) The projected-DOS of (a) RS CoO and (b) AF3 phase of WZ CoO. Dotted (blue) and solid (red) lines represent the states projected onto the Co and O sites, respectively. The Fermi level is set to be zero (vertical dotted line).

To verify the other possibility, we also performed total energy calculations for the several uncompensated AFM configurations that carry the net moments. Note that these are rather artificial spin orders because they are not commensurate with the unitcell. They are found to have significantly higher energies compared to the most stable AF3 by 0.018–0.022 eV/CoO. Thus, such unnatural spin orders carrying net moments can also be ruled out as the source of the observed moment Ref. 15.

The relative stability of these collinear spin configurations can be understood by counting the number of AFM and FM couplings, as summarized in Table I. Since the bond angles between Co ions are approximately 110° , AFM couplings are probably favored. Thus, the configuration that maximizes the number of AFM pairs (and minimizes FM pairs), would

become most stable. As shown in Table I, this is the case for AF1 and AF3. AF2a and AF4 have higher energies than AF1 and AF3 by 7–10 meV/CoO due to their fewer AFM (and more FM) couplings. Although AF2b has the same number of AFM pairs as AF2a and AF4, all of its AFM pairs are along the out-of-plane direction. Thus, its higher total energy reflects the different in-plane magnetic interactions from the out-of-plane ones. Our simple rule of nearest-neighbor number counting is further confirmed by the fact that AF1 and AF2a have almost same energy as AF3 and AF4, respectively; they actually have the same number of nearest-neighbor FM/AFM couplings. The small energy differences, ~ 0.001 eV/CoO, can reflect the effect from the longer range interactions.

From the calculated total energies, we estimated the exchange coupling parameter in the Heisenberg spin Hamiltonian, $H_{ij} = -J \sum S_i S_j$. Considering the number of AFM and FM couplings shown in Table I, the in-plane and out-of-plane interactions as can be calculated follows:

$$J_{\text{in}}^{\text{WZ}} = \frac{1}{4}(E_{\text{tot}}^{1,3} - \frac{1}{2}E_{\text{tot}}^{2a,4}) = -3 \text{ meV}, \quad (1)$$

$$J_{\text{out}}^{\text{WZ}} = \frac{1}{4}(E_{\text{tot}}^{1,3} - \frac{1}{12}E_{\text{tot}}^{2b}) = -1 \text{ meV}. \quad (2)$$

In these equations, E_{tot}^m represents the calculated total energy (per CoO) for the spin configuration (denoted by m), and we used $S = \pm 1.5$ for Co spin which is in good agreement with the calculated moment. The estimated AFM interactions for both in-plane and out-of-plane spin directions are consistent with the total energy results shown in Table I: *e.g.*, AF2b phase, is less stable than AF2a and AF4 because $|J_{\text{in}}| < |J_{\text{out}}|$ (see, Fig. 1 and Table I). Note that the nearest-neighbor couplings are AFM, which can be supported also by the Monte Carlo calculations [22, 23]. The difference between the coupling strengths in Ref. 22 and our results reflects the different spin structures assumed in the two studies. It is useful to compare our result with the hypothetical WZ MnO case reported by Gopal *et al.* [36]: The in-plane and out-of-plane couplings for WZ MnO are $J_{\text{in}}^{\text{MnO}} = -3.7$ meV and $J_{\text{out}}^{\text{MnO}} = -4.5$ meV, respectively [37]. It is noted that they are also AFM along both directions and with the same order of magnitude, whereas in MnO the out-of-plane coupling is stronger than the in-plane one. It should be noted that the J values in WZ-MnO were estimated based on the LSDA ($U = 0$) total energies, which can produce a substantial difference from LDA+ U results.

The electronic structure of WZ CoO is different from conventional RS CoO owing to its

tetrahedral crystal field. Since Co^{2+} ions are located in the oxygen tetrahedra instead of the octahedra, their $3d$ levels are split into low-lying e and higher t_2 bands [14, 21], with seven electrons occupying the up-spin e^\uparrow and t_2^\uparrow bands and the down-spin e^\downarrow bands. It is consistent with the calculated Co magnetic moment $\sim 3\mu_B$. The projected densities-of-states (PDOS) for the most stable AF3 are shown and compared to those in RS phase in Fig. 2. The band dispersion is presented in Fig. 3 where the orbital characters are represented by shape and size of the symbols. While the band structure is quite similar to that of the c -type AFM phase obtained by LDA+ U in Ref. 21, it is clearly different from the LSDA ($U=0$) results in Ref. 14. The finite gap and large exchange splitting are attributed to the on-site correlation, U , which cannot be well captured by the LSDA ($U = 0$) [14]. Also, the LDA+ U valence bands are dominated by the O-2 p and Co-3 d mixture whereas the LSDA bands are of mainly Co character [14].

Finally, we note that in WZ structure, Co spins form hexagonal networks and their exchange couplings are all AFM as discussed above. It suggests that collinear spin arrangements may not be well stabilized, but a non-collinear order is realized. For the further examination of magnetic ground states, the relativistic calculations including spin-orbit couplings were performed. We constructed commensurate non-collinear spin structures by enlarging our unitcell to contain 24 atoms (see Fig. 4). All spins are assumed to align in the ab -plane, which is supported by a recent Monte Carlo calculation [23]. Within this unitcell, four different non-collinear configurations can be considered, namely Γ_1 – Γ_4 (see Fig. 4). The configurations are distinguishable by their topologies, as shown in Fig. 4(b), while all the angles between in-plane spins are 120° . Note that all the configurations, Γ_1 – Γ_4 , carry zero total moments.

Total energy calculations show that the non-collinear spin structures are more stable than the collinear configurations. The collinear spin orders have higher energies than the non-collinear configurations by more than 21 meV although this energy difference can be as small as $\sim \pm 0.1$ meV/CoO depending on the details of computation such as the anisotropy of spin direction, spin-orbit coupling, and the constraints in the non-collinear calculations. Therefore, our results demonstrate that a novel non-collinear spin ordering can be realized in CoO nanostructures. Γ_3 is found to be most stable among the non-collinear configurations, whereas Γ_1 has almost same energy as Γ_3 ; the difference between the two is $E(\Gamma_1 - \Gamma_3) = 0.02$ meV/CoO. Γ_2 and Γ_4 have higher energies than Γ_1 and Γ_3 by 7.28 and 7.34 meV/CoO,

respectively.

This type of non-collinear spin order has not been found in TMO nanostructures. We also emphasize that this novel spin ground state becomes stabilized through the structural transformation caused by a material-size reduction into the nano-meter scale, which can add a new interesting aspect to nano-magnetism studies. We hope that this work stimulates further research efforts from both experimental and theoretical perspectives.

IV. CONCLUSION

Magnetic properties of WZ structure CoO often appearing in CoO nanocrystals have been studied by using LDA+ U density functional method. Total energy calculations show that the novel non-collinear spin order can be stabilized, whereas so-called AF3 type is the most stable among the collinear spin configurations. Non-collinear spin structures stabilized in the nano-meter scale are expected to provide a new aspect to nano-magnetism studies.

V. ACKNOWLEDGMENTS

We are grateful to Prof. T. Ozaki and Dr. B.-J. Yang for discussions. This work was supported by the NRF through ARP (Grant No. R17-2008-033-01000-0). This work was supported by the National Institute of Supercomputing and Networking / Korea Institute of Science and Technology Information with supercomputing resources including technical support (KSC-2013-C2-005).

-
- [1] S. Sun, C. B. Murray, D. Weller, L. Folks, and A. Moser, *Science* **287**, 1989 (2000);
 - [2] D. D. Awschalom and D. P. DiVincenzo, *Phys. Today*, **48**(4), 43 (1995);
 - [3] J. Park, K. J. An, Y. S. Hwang, J. G. Park, H. J. Noh, J. Y. Kim, J. H. Park, N. M. Hwang, T. Hyeon, *Nature Mater.* **3** 891 (2004).
 - [4] I. M. L. Billas, A. Chatelain, and W. A. de Heer, *Science* **265**, 1682 (1994).
 - [5] S. -W. Kim, M. Kim, W. Y. Lee, and T. Hyeon, *J. Am. Chem. Soc.* **124**, 7642 (2002);
 - [6] S. -W. Kim, S. U. Son, S. S. Lee, T. Hyeon, and Y. K. Chung, *Chem. Commun.* **2001**, 2212 (2001).

- [7] J. Li, Y. J. Wang, B. S. Zou, X. C. Wu, J. G. Lin, L. Guo, and Q. S. Li, Appl. Phys. Lett. **70**, 3047 (1997).
- [8] G. H. Lee, S. H. Huh, J. W. Jeong, B. J. Choi, S. H. Kim, and H. -C. Ri, J. Am. Chem. Soc **124**, 12094 (2002).
- [9] W. S. Seo, H. H. Jo, K. Lee, B. Kim, S. J. Oh, and J. T. Park, Angew. Chem. Int. Ed. **43**, 1115 (2004).
- [10] J. Park, E. Kang, C. J. Bae, J.-G. Park, H.-J. Noh, J.-Y. Kim, J.-H. Park, H. M. Park, and T. Hyeon, J. Phys. Chem. B **108**, 13594 (2004).
- [11] M. J. Han, T. Ozaki, and J. Yu, J. Chem. Phys. **123**, 034306 (2005).
- [12] E. Tronc, C. Chaneac, and J. P. Jolivet, J. Solid State Chem. **139**, 93 (1998).
- [13] W. S. Seo, J. H. Shim, S. J. Oh, E. K. Lee, N. H. Hur, and J. T. Park, J. Am. Chem. Soc. **127**, 6188 (2005).
- [14] A. S. Risbud, L. P. Snedeker, M. M. Elcombe, A. K. Cheetham, and R. Seshadri, Chem. Mater. **17**, 834 (2005).
- [15] K. An, N. Lee, J. Park, S. C. Kim, Y. Hwang, J.-G. Park, J.-Y., Kim, J.-H. Park, M. J. Han, J. Yu, and T. Hyeon, J. Am. Chem. Soc. **128**, 9753 (2006).
- [16] M. Venkatesan, C. B. Fitzgerald, J. G. Lunney, J. M. D. Coey, Phys. Rev. Lett. **93**, 177206 (2004).
- [17] A. J. Behan, A. Mokhtari, H. J. Blythe, D. Score, X.-H. Xu, J. R. Neal, A. M. Fox, and G. A. Gehring, Phys. Rev. Lett. **100**, 047206 (2008).
- [18] K. R. Kittilstved, N. S. Norberg, and D. R. Gamelin, Phys. Rev. Lett. **94**, 147209 (2005).
- [19] M. Bouloudenine, N. Viart, S. Colis, J. Kortus, and A. Dinia, Appl. Phys. Lett. **87**, 052501 (2005).
- [20] S. Deka, R. Pasricha, and P. A. Joy, Phys. Rev. B **74**, 033201 (2006).
- [21] M. J. Han and J. Yu, J. Korean Phys. Soc. **48**, 1496 (2006).
- [22] T. Archer, R. Hanafin, and S. Sanvito Phys. Rev. B **78**, 014431 (2008).
- [23] R. Hanafin, T. Archer, and S. Sanvito Phys. Rev. B **81**, 054441 (2010).
- [24] V. I. Anisimov, F. Aryasetiawan, and A. I. Lichtenstein, J. Phys.:Condens. Matter **9**, 767 (1997).
- [25] T. Ozaki, Phys. Rev. B. **67**, 155108, (2003); T. Ozaki and H. Kino, Phys. Rev. B **69**, 195113, (2004); T. Ozaki and H. Kino, J. Chem. Phys. **121**, 10879, (2004).

- [26] M. J. Han, T. Ozaki, and J. Yu, Phys. Rev. B **73**, 045110 (2006).
- [27] D. M. Ceperley and B. J. Alder, Phys. Rev. Lett. **45**, 566 (1980); J. P. Perdew and A. Zunger, Phys. Rev. B **23**, 5048 (1981).
- [28] N. Troullier and J. L. Martins, Phys. Rev. B **43**, 1993 (1991).
- [29] S. G. Louie, S. Froyen, and M. L. Cohen, Phys. Rev. B **26**, 1738 (1982).
- [30] P. E. Blöchl, Phys. Rev. B **41**, R5414 (1990).
- [31] J. Junquera, O. Paz, D. Sanchez-Portal, and E. Artacho, Phys. Rev. B **64**, 235111 (2001); J. M. Soler, E. Artacho, J. D. Gale, A. Garcia, J. Junquera, P. Ordejon, and D. Sanchez-Portal, J. Phys.:Condens. Matter **14**, 2745 (2002) and references therein.
- [32] T. Ozaki and H. Kino, Phys. Rev. B **72**, 045121, (2005).
- [33] A. H. MacDonald and S. H. Vosko, J. Phys. C: Solid State Phys. **12**, 2977 (1979); G. Theurich and N. A. Hill, Phys. Rev. B. **64**, 073106 (2001); G. B. Bachelet, D. R. Hamann, and M. Schluter, Phys. Rev. B. **26**, 4199 (1982).
- [34] All the DFT calculations were performed using our DFT code, OpenMX (<http://openmx-square.org>).
- [35] Same type of classification was applied to the WZ structure MnS: see, R. I. Hines, N. L. Allan, G. S. Bell, and W. C. Mackrodt, J. Phys.: Condens. Matter. **9**, 7105 (1997).
- [36] P. Gopal, N. A. Spaldin, and U. V. Waghmare, Phys. Rev. B. **70**, 205104 (2004).
- [37] It should be noted that Gopal *et al.* took the spin value of $S = \pm 1$ and obtained $J_{\text{in}}^{\text{MnO}} = -23$ meV and $J_{\text{out}}^{\text{MnO}} = -28$ meV in Ref. 36. We present the normalized J values by taking $S^{\text{MnO}} = \pm 2.5$ for comparison.

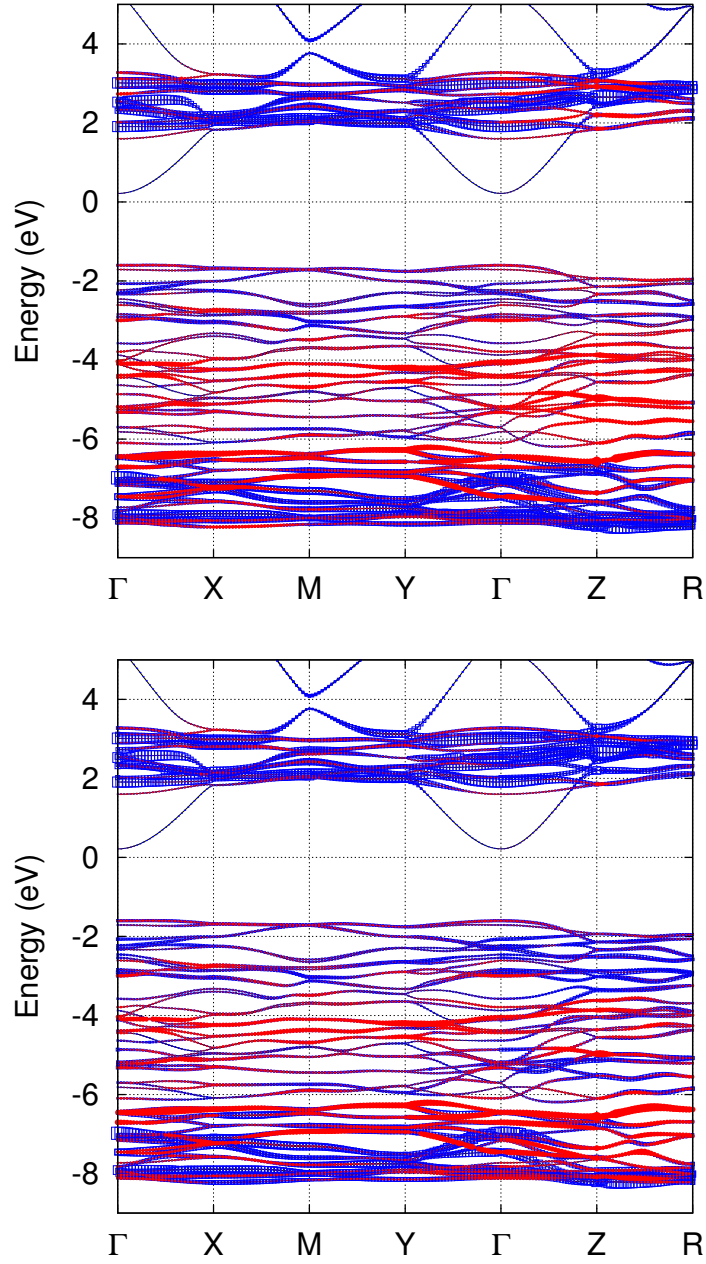


FIG. 3: (Color online) The calculated fat-band dispersion. The upper and lower panel represent the up and down spin bands, respectively. The blue-boxes and red-circles represent the t_{2g} (t_2) and e_g (e) components with the symbol size proportional to the weight of each component.

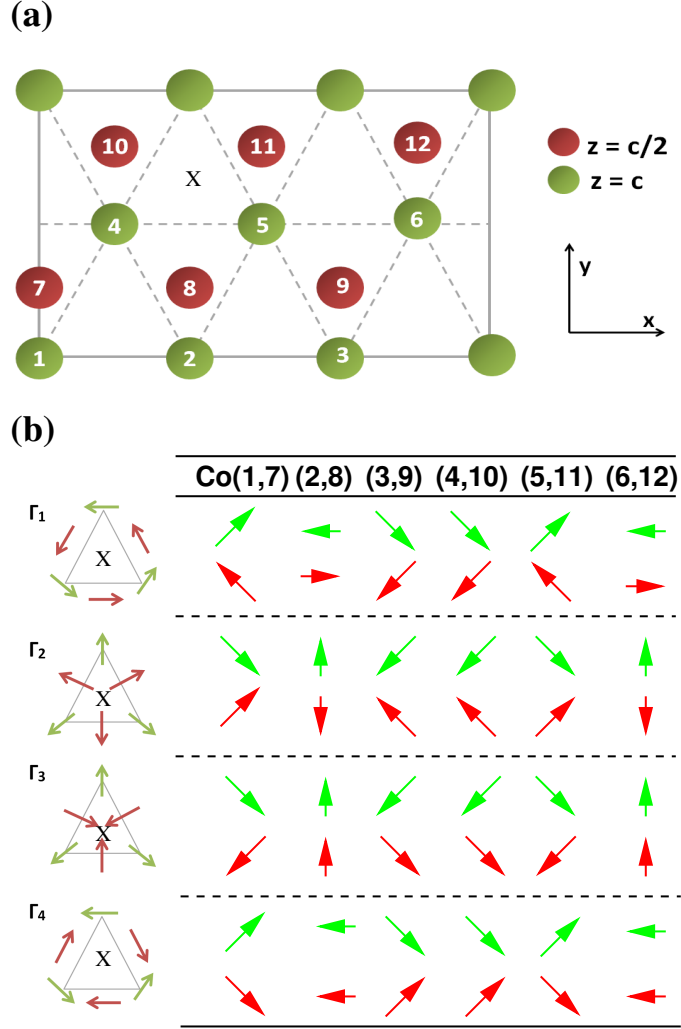


FIG. 4: (Color online) Unicell spin structures for non-collinear configurations. Bright (green) and dark (red) circles in (a) and arrows in (b) represent the Co atoms at $z = 0, c$ and $z = \frac{1}{2}c$ plane, respectively. The arrows in (b) indicate the spin direction within the ab -plane.